The Local Ordering of Molten $LiNbO_3$ by X-ray Diffraction

K. Sugiyama, K. Nomura, and Y. Waseda

Research Institute of Mineral Dressing and Metallurgy (SENKEN), Tohoku University, Sendai 980, Japan

P. Andonov* and S. Kimura

National Institute for Research in Inorganic Materials, 1–1 Namiki, Tsukuba 305, Japan

K. Shigematsu

Faculty of Education, Iwate University, Morioka 020, Japan

Z. Naturforsch. **45a**, 1325–1327 (1990); received July 19, 1990

The structure of molten $LiNbO_3$ has been studied in the range 1550–1600 K by high temperature X-ray diffraction. Octahedrally coordinated niobium is suggested to exist in the melt as a fundamental local structure.

$LiNbO_3$ crystal has excellent electro-optical and non-linear optical properties [1, 2]. However local fluctuations of the refractive index and light scattering centers prevent a wider application of this material in optical devices. Since sub-grain boundaries seem to cause such inconvenience, the production of sub-grain free $LiNbO_3$ crystals is strongly required. Various properties of molten $LiNbO_3$, such as viscosity, density, and surface tension have recently been measured in order to understand the growth of $LiNbO_3$ single crystals in the Czochralski method [3, 4]. The viscosity of molten $LiNbO_3$ is relatively high just above the melting point (1526 K) and then decreases strongly in the range up to 1553 K [4]. A similar anomalous behaviour has been detected for other physical properties of molten $LiNbO_3$ and may be related to the appearance of subgrain boundaries during the growth of $LiNbO_3$ crystals from the melt [4]. The structure of molten $LiNbO_3$ seems not to have been studied as yet. This prompted us to present our results obtained with a high temperature X-ray diffraction method.

A miniature furnace composed of four small silicon carbide ceramic heaters in a refractory brick (Fig. 1) used for our measurements. This furnace, set in a high temperature chamber as described in detail in [5], made it possible to maintain the sample temperature within ± 10 K at a desired temperature below 1673 K. Single crystal flakes of $LiNbO_3$, provided by Mitsui Mining and Smelting Co. Ltd., were charged into a platinum container ($30 \times 20 \times 5$ mm^3) settled in the center of the furnace. The sample temperature was monitored by a Pt-Pt 13% Ph thermocouple inserted just below the platinum container. A sufficiently flat surface of the sample was expressively certified.

X-ray scattering intensities from the molten $LiNbO_3$ sample at 1548, 1573, and 1598 K in air were measured using a theta-theta diffractometer which allowed the

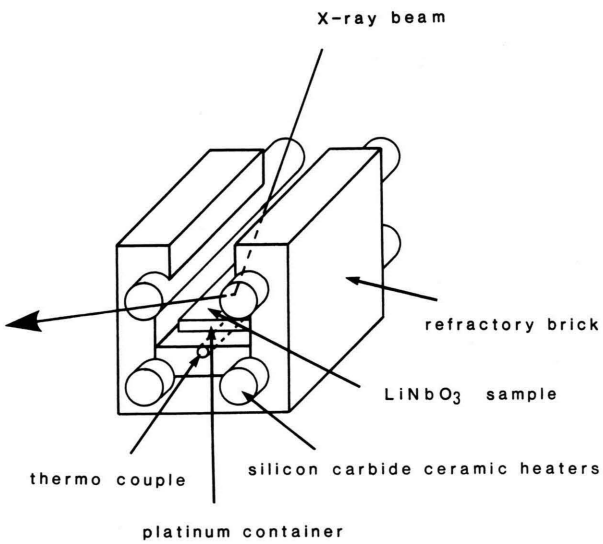

Fig. 1. Schematic diagram of a miniature furnace prepared in the present work.

* Permanent address: Laboratoire de Magnetisme du C.N.R.S. 1 place Austide Briand, 92195 Meudon Cedex, France.

Reprint requests to Dr. K. Sugiyama, Research Institute of Mineral Dressing and Metallurgy, SENKEN, Tohoku University, Sendai 980, Japan.

0932-0784 / 90 / 1100-1325 $ 01.30/0. – Please order a reprint rather than making your own copy.

Dieses Werk wurde im Jahr 2013 vom Verlag Zeitschrift für Naturforschung in Zusammenarbeit mit der Max-Planck-Gesellschaft zur Förderung der Wissenschaften e.V. digitalisiert und unter folgender Lizenz veröffentlicht: Creative Commons Namensnennung-Keine Bearbeitung 3.0 Deutschland Lizenz.

This work has been digitalized and published in 2013 by Verlag Zeitschrift für Naturforschung in cooperation with the Max Planck Society for the Advancement of Science under a Creative Commons Attribution-NoDerivs 3.0 Germany License.

Zum 01.01.2015 ist eine Anpassung der Lizenzbedingungen (Entfall der Creative Commons Lizenzbedingung „Keine Bearbeitung") beabsichtigt, um eine Nachnutzung auch im Rahmen zukünftiger wissenschaftlicher Nutzungsformen zu ermöglichen.

On 01.01.2015 it is planned to change the License Conditions (the removal of the Creative Commons License condition "no derivative works"). This is to allow reuse in the area of future scientific usage.

sample to be held in a stationary horizontal position and the X-ray tube and detector rotated in opposite directions [5]. The intensity profile was obtained using a molybdenum X-ray tube and a singly-bent pyrolitic graphite monochromator in the diffracted beam in the angular range from 2° to 50°, which corresponds to the wave vectors $Q=4\pi \sin \Theta/\lambda$ from 6 to 135 nm^{-1}, where λ is the wave length and 2Θ the angle between the incident and diffracted X-ray beam. The observed intensity data at $Q<6\ nm^{-1}$ were smoothly extrapolated to zero at $Q=0\ nm^{-1}$. The effect of this extrapolation or truncation up to $Q=135\ nm^{-1}$ for the broad peaks observed in a liquid sample is known to make no critical contribution to the radial distribution function (RDF) calculated from the coherent scattering intensity if only $Q>70\ nm^{-1}$ [6].

The method of analyzing the measured X-ray scattering intensity for non-crystalline systems is well known [6, 7]. In order to convert the measured scattering intensity into the coherent scattering intensity $I_{eu}^{coh}(Q)$, the generalized Krogh-Moe-Norman method [8] was used with atomic form factor including the anomalous dispersion corrections [9]. The Compton scattering was corrected using the values reported by Smith Jr. et al. [10]. The RDF of $4\pi r^2 \varrho(r)$ for a non-crystalline system containing more than two kinds of atoms can be estimated from $I_{eu}^{coh}(Q)$ by the equation

$$4\pi r^2 \varrho(r) = 4\pi r^2 \varrho_0 + \frac{2r}{\pi} \int_0^\infty Q \frac{[I_{eu}^{coh}(Q) - \langle f^2 \rangle]}{\langle f \rangle^2} \sin(Qr)\, dQ, \quad (1)$$

where $\langle f \rangle$ is the average atomic scattering factor and $\langle f^2 \rangle$ is the mean square of the atomic scattering factor. $\varrho(r)$ is the average radial density function and ϱ_0 is the average number density of atoms.

Figure 2 shows the obtained coherent scattering intensities. No particular change with temperature is detected in these three patterns, except for a shoulder on the higher Q side of the first peak appearing at the low temperature. The RDFs were calculated using (1) with density values from [4]. Again no significant structural change with temperature appears in the calculated RDFs. The RDF for 1573 K is given in Fig. 3 as an example. The arrows indicate the position of some atomic pairs in crystalline $LiNbO_3$ [11]. Only atomic correlations such as Nb–O and Nb–Nb can be discussed because the electron numbers of lithium and oxygen are very small (3 and 8, respectively) compared to that of niobium (41). The peak around

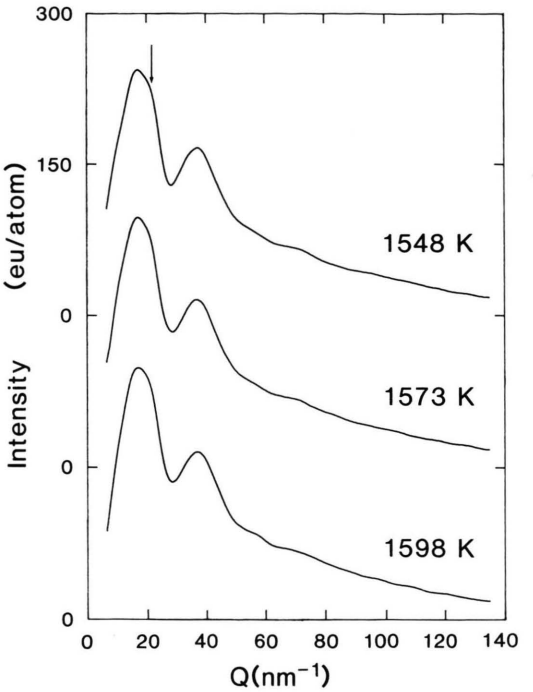

Fig. 2. The coherent scattering intensities $I_{eu}^{coh}(Q)$ of molten $LiNbO_3$ at 1548, 1573 and 1598 K. A shoulder at about $Q=21\ nm^{-1}$, indicated by an arrow, appears as the melting point is approached.

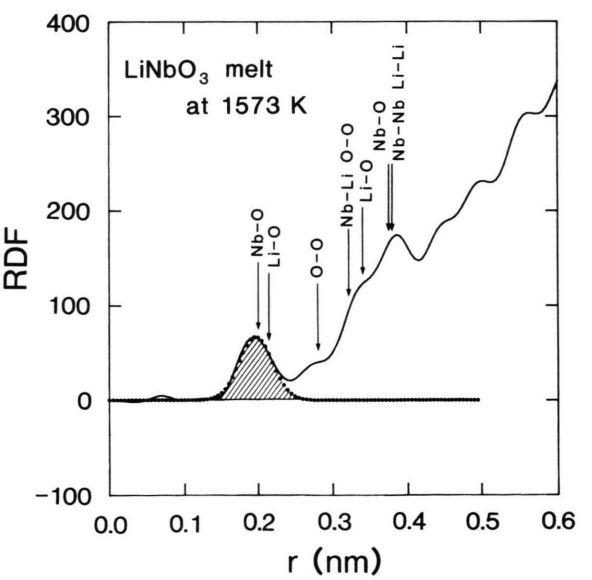

Fig. 3. Radial distribution function of molten $LiNbO_3$ at 1573 K. The arrows indicate the positions of some atomic pairs estimated from the crystalline structure of $LiNbO_3$ [11]. The shaded area denotes the first coordination shell for a Nb–O pair assuming the Gaussian form.

0.2 nm was attributed to the Nb–O pair, and the peak position and coordination number were estimated to be 0.197 nm and 5.8, respectively. The nearest Nb–O correlation in molten $LiNbO_3$ is comparable to that in crystalline $LiNbO_3$ (0.200 nm and 6.0, respectively). The error in the coordination number in this work being of the order of $\pm 10\%$, the present authors maintain that the local unit structure of molten $LiNbO_3$ is quite similar to that of the octahedrally coordinated niobium in the crystal. The peak around 0.38 nm could be attributed to the Nb–Nb pair from the structure of crystalline $LiNbO_3$ [11]. However, the limited accuracy of the present RDF data prevents us from quantitatively determining the coordination number of Nb–Nb pairs.

Although any drastic change with temperature in the structure of molten $LiNbO_3$ is not evident from the present X-ray diffraction data, the shoulder appearing at about $Q = 21\ nm^{-1}$ near the peak around $Q = 17\ nm^{-1}$ is noteworthy. This wave vector region corresponds mainly to the contribution from the second neighbouring Nb–Nb pairs, based on the usual crystallographic analysis. Therefore, the appearance of the shoulder may be related to a change of association in molten $LiNbO_3$, and this may have to do with the particular behaviour of various properties of molten $LiNbO_3$ near the melting point.

The authors gratefully acknowledged for the financial support from Special Coordination Fund for Promotion of Science and Technology granted for "Study of Macro-clusters in Melt and their Influence to Crystal Growth".

[1] A. A. Ballman, J. Amer. Ceram. Soc. **48,** 112 (1965).
[2] A. Fedolov, Z. I. Shapiro, and P. B. Ladyzhinskii, Sov. Phys. Crystallogr. **10,** 218 (1865).
[3] S. A. Bol'shkov, V. P. Klyuev, N. N. Lyapushkin, A. P. Lyubimov, and S. A. Fedulov, Inorg. Mat. **5,** 824 (1969).
[4] K. Shigematsu, Y. Anzai, S. Morita, M. Yamada, and H. Yokoyama, Japanese J. Appl. Phys. **26,** 1988 (1987).
[5] Y. Waseda, K. Hirata, and M. Ohtani, High Temp. High Pressures **7,** 221 (1975).
[6] K. Furukawa, Rep. Prog. Phys. **25,** 395 (1962).
[7] See for example: H. P. Klug and L. E. Alexander, X-ray Diffraction Procedures for Polycrystalline and Amorphous Materials, 2nd edition, John Wiley & Sons, New York 1974.
[8] C. N. J. Wagner, H. Ocken, and M. J. Joshi, Z. Naturforsch. **20a,** 325 (1965).
[9] International Tables for X-ray Crystallography, Vol. IV, The Kynoch Press, Birmingham 1974.
[10] V. H. Smith Jr., A. J. Thakkar, and D. C. Chapman, Acta Cryst. **A 31,** 391 (1975).
[11] S. C. Abrahams, J. M. Reddy, and J. L. Bernstein, J. Phys. Chem. Solids **27,** 997 (1966).